Received: 25 January 2022 | Accepted: 8 March 2022

DOI: 10.1002/jcc.26849

RESEARCH ARTICLE

Journal of COMPUTATIONAL CHEMISTRY WILEY

Effects of oxidative adsorbates and cluster formation on the electronic structure of nanodiamonds

Thorren Kirschbaum[1,2] | Tristan Petit[3] | Joachim Dzubiella[1,4] | Annika Bande[5]

[1]Simulation of Energy Materials, Helmholtz-Zentrum Berlin für Materialien und Energie GmbH, Berlin, Germany

[2]Artificial Intelligence for the Sciences, FB Mathematik und Informatik, Freie Universität Berlin, Berlin, Germany

[3]Nanoscale Solid-Liquid Interfaces, Helmholtz-Zentrum Berlin für Materialien und Energie GmbH, Berlin, Germany

[4]Applied Theoretical Physics—Computational Physics, Physikalisches Institut, Albert-Ludwigs-Universität Freiburg GmbH, Freiburg, Germany

[5]Theory of Electron Dynamics and Spectroscopy, Helmholtz-Zentrum Berlin für Materialien und Energie GmbH, Berlin, Germany

Correspondence
Annika Bande, Theory of Electron Dynamics and Spectroscopy, Helmholtz-Zentrum Berlin für Materialien und Energie GmbH, Hahn-Meitner-Platz 1, 14109 Berlin, Germany.
Email: annika.bande@helmholtz-berlin.de

Funding information
Zentraleinrichtung für Datenverarbeitung (ZEDAT) of Freie Universität Berlin; Helmholtz Einstein International Berlin Research School in Data Science (HEIBRiDS)

Abstract

Nanodiamonds (NDs) are modern high-potential materials relevant for applications in biomedicine, photocatalysis, and various other fields. Their electronic surface properties, especially in the liquid phase, are key to their function in the applications, but we show that they are sensitively modified by their interactions with the environment. Two important interaction modes are those with oxidative aqueous adsorbates as well as ND self-aggregation towards the formation of ND clusters. For planar diamond surfaces it is known that the electron density migrates from the diamond towards oxidative adsorbates, which is known as transfer doping. Here, we quantify this effect for highly curved NDs of varying sizes (35–147 C atoms) and surface terminations (H, OH, F), focusing on their interactions with the most abundant aqueous oxidative adsorbates (H_3O^+, O_2, O_3). We prove that the concept of transfer doping stays valid for the case of the high-curvature NDs and can be tuned via the ND's specific properties. Secondly, we investigate the electronic structures of clusters of NDs which are known to form in particular in aqueous dispersions. Upon cluster formation, we find that the optical gaps of the structures are significantly reduced, which explains why different experimental values were obtained for the optical gap of the same structures, and the cluster's LUMO shapes resemble atom-type orbitals, as in the case of isolated spherical NDs. Our findings have implications for ND applications as photocatalysts or electronic devices, where the specific electronic properties are key to the functionality of the ND material.

KEYWORDS
clusters, DFT, molecular modeling, nanodiamonds, transfer doping

1 | INTRODUCTION

Diamond-based materials provide very high stability, hardness, biocompatibility, and notable electronic properties such as the ability for negative electron affinity (NEA).[1] The discovery of these unique characteristics has led to various applications in science and technology, i.e., as electronic devices.[2–4] In the field of nanomaterials, nanodiamonds (NDs) are used in catalysis,[5,6] biomedicine,[7–9] energy materials[10] and many more.[1,11–13] For catalysis and biomedicine, the NDs are usually dispersed in aqueous media, hence, effects of the condensed environment on the NDs are of high importance for these fields.

Diamond is usually considered as an inert material due to a very stable sp^3-coordinated carbon core. However, when shrinking its size, surface effects dominate and electronic interaction of NDs with their environment can strongly influence their properties, which needs to

be considered for better anticipation of their properties. In a previous study, Aranifard and Shojaei investigated the interaction of neutral, protonated and deprotonated water clusters with the bare and functionalized ND C_{35}. They reported especially strong hydrophobic interactions with bare C_{35} and OH^-, and significant rearrangement of electron density when charged water clusters are in contact with bare C_{35}.[14] In the present article, we extend the theoretical investigations by quantifying and explaining the charge migration between NDs and aqueous oxidative adsorbates for different ND sizes, ND surface terminations and adsorbates. Furthermore, we investigate the electronic interactions between several cluster-forming diamondoids.

The interaction of bulk diamond surfaces with aqueous adsorbates has been extensively researched, especially because hydrogen-terminated diamond surfaces display unique properties when in contact with ambient water. In 1989, Landstrass and Ravi demonstrated that hydrogen plasma-treated diamond has a surface conductivity which is increased by several orders of magnitude as compared to the untreated substrate.[15] This was later corroborated by Shiomi et al.[16] In 2007, Chakrapani et al.[17] established that this increased surface conductivity is induced by carrier hole doping: In the presence of air-equilibrated water, electrons move from the diamond surface into the liquid phase where they drive the redox reaction $O_2 + 4H^+ + 4\,e^- \rightleftharpoons 2\,H_2O$. When oxygen is purged from the water, no electron flow occurs. However, if the water pH is lowered, electrons again move from the H-terminated diamond surface into the acidic water.[17] This effect, now known as transfer doping, has concurrently been studied in many experimental[17–21] and theoretical works,[22–29] however, until now, such investigations are missing for the case of NDs. Especially, O_3 in aqueous solution has been proposed to remove inhomogeneities from the diamond surface and obtain a fully O-functionalized surface.[30] To understand this process a better understanding of O_3-ND interaction in water is desirable.

Furthermore, it is known from experiments that NDs tend to form clusters and self-assembled networks in solution.[31,32] Theoretical work has been conducted on the aggregation behavior[32] and stability[33] of those clusters as well as on the electronic properties of single isolated NDs,[34] but the effects of cluster formation on the NDs' electronic properties are so far unexplored.

The surface chemistry of diamond can dramatically tune its electronic properties (electron affinity, work function, reactivity, etc.) without modifying the bulk material. This effect is amplified with NDs due to their large surface area, which can be used for many applications. For example, NDs covered by hydrogen, fluorine or hydroxyl species will have radically different surface electronic properties.[35–38]

In this study, we quantify the effect of surface transfer doping for NDs of different sizes (35–147 carbon atoms) and three surface modifications (H, F, OH). The aqueous oxidative adsorbates include $H_2O{\cdot}H_2O$, $H_3O^+{\cdot}H_2O$, $O_2{\cdot}H_2O$ and $O_3{\cdot}H_2O$, as these are the most abundant species in water and were already investigated in previous work on the diamond (100) surface.[28] In the second part of the study, we investigate the impact of cluster formation on the electronic properties of the smallest NDs, the diamondoids. In the diamondoid series, the smallest molecule (adamantane) consists of only one cage of tetrahedrally coordinated carbon atoms terminated by hydrogen. The higher diamondoids can be built from this structure by subsequentially adding further diamond cages to the adamantane structure, leading to diamantane, triamantane, and so on. All of these structures are H-terminated fragments of the diamond crystal lattice. For these molecules (monomers), experimental data on their electronic structure (i.e., the optical gap) is available.[39–41] With our computations of the electronic structure of diamandoid clusters, we clarify why different optical gaps have been obtained from optical absorption experiments in the gas phase[39,40] and from X-ray emission/absorption studies on diamondoid powders,[41] and we investigate the clusters' frontier orbital shapes.

2 | THEORETICAL METHODS

The structures of aqueous molecular adsorbates on NDs were optimized using the Perdew-Burke-Ernzerhof (PBE) general-purpose functional[42] and Ahlrich's def2-SVP basis set.[43,44] Here, we have resorted to the simple PBE GGA functional and the small basis set to make the geometry optimizations of large structures feasible. Subsequently, single-point calculations were performed on these structures to obtain precise electronic properties using the hybrid meta-GGA TPSSH functional[45,46] and Ahlrich's def2-TZVP basis set. The TPSSH functional was proven to yield accurate results both for general main group DFT calculations[47] and in particular for the calculation of diamondoids' electronic properties.[48] In the single point calculations, we added an implicit solvent model (conductor-like polarizable continuum model, CPCM)[49] to simulate the surrounding water shell, and we used the fractional occupation number weighted electron density (FOD) method[50] to allow for fractional occupation numbers of molecular orbitals at finite temperatures, according to the effect of electron density migration under study. Charge migration was quantified by calculating the total Hirshfeld charges of the molecular adsorbates, which has previously been applied in similar work.[28] We found the same trends when using Loewdin charge analysis instead. We also found that different minimum energy geometric arrangements of the adsorbates have only minor effects on the quantity of the charge migration. Therefore, in the cases where several calculations were conducted for the same system, we report values for one representative structure.

The diamondoid monomer, dimer, and cluster structures were optimized via TPSSH and Ahlrichs' minimally augmented def2-SVP basis set. The non-augmented basis set was already used successfully to calculate the electronic properties of diamondoids,[51] however, we included minimal augmentation to better describe the delocalized, spread-out lowest unoccupied molecular orbitals (LUMOs) of the clusters.[48] Note that the use of augmented basis sets was not feasible for the larger structures in the first part of the study. It is known that alone for the adamantane dimer more than 20 local minimum structures exist within 2 kJ/mol of the putative global minimum,[33] however, slight changes in the structures' geometries did not have a significant impact on the properties presented herein. The diamondoids' HOMO-LUMO gap (HLG) values were corrected

according to the zero-point energy gap renormalizations (ZPR) as calculated by Han et al.[52] For the dimers and higher adamantane clusters, no ZPR corrections have been calculated explicitly, but we use the respective monomer corrections as a proxy instead. We also tested for possible errors induced by basis set superposition, but found the deviations to be negligible.

In all calculations, Grimme's third order atom-pairwise dispersion correction with Becke-Jones (D3BJ) dampening was used.[53] For calculations involving TPSSH, the RIJCOSX approximation[54] together with the appropriate auxiliary basis sets[55] was employed to speed up integral calculation. The ORCA program package, version 4.2.1, was used throughout.[56]

3 | RESULTS AND DISCUSSION

3.1 | Nanodiamonds: electron transfer doping

The effect of transfer doping describes the migration of electronic charge density from the diamond material towards an aqueous adsorbate in the ground state.[17] We investigate this phenomenon for the four most abundant aqueous oxidative adsorbates ($H_2O{\cdot}H_2O$, $H_3O^+{\cdot}H_2O$, $O_2{\cdot}H_2O$, $O_3{\cdot}H_2O$) on NDs of different sizes ($C_{35}H_{36}$, $C_{53}H_{48}$, $C_{84}H_{64}$, $C_{147}H_{100}$) and surface terminations ($C_{84}H_{64}$, $C_{84}[OH]_{64}$ and $C_{84}F_{64}$). For each series of calculations, one parameter is varied (adsorbate/ND size/ND surface) while the other two parameters are fixed to the default setting $C_{84}H_{64}{\cdot}O_2{\cdot}H_2O$, respectively.

In Table 1 we report the electron transfer (ET) for the different adsorbates on the ND $C_{84}H_{64}$ which has an octahedral shape with eight facets of (111) surfaces, a typical ND shape.[57] The corresponding structures are shown in Figure 1. No significant effect is observed for the adsorbed water only, but a charge transfer from the ND to the adsorbates of 0.21 e ($H_3O^+{\cdot}H_2O$) to 0.51 e ($O_3{\cdot}H_2O$) is induced once an oxidative adsorbate is present. The magnitudes of ET correlate with the chemical potentials of the adsorbates which are both in the order $H_2O{\cdot}$ H_2O < H_3O^+ < O_2 < O_3.[28,58] This corroborates the observation that the electrons move towards the oxidative adsorbate to drive the respective redox reaction in the aqueous phase. When aqueous ozone is used as an oxidizing agent for H-terminated NDs, the holes that are formed in the NDs upon surface transfer doping may add to the reactivity of the system and result in faster oxidation reactions.[30] The magnitude of charge migration depends on the electrochemical standard potential of the respective reaction which is

TABLE 1 Electron transfer (ET) from ND $C_{84}H_{64}$ towards varying adsorbates, quantified by the transferred Hirshfeld charge in elemental unit charge e (PBE-D3/SVP geometries, TPSSH-D3/TZVP/CPCM[water] single point calculations)

ND	Adsorbates	ET/e
$C_{84}H_{64}$	$H_2O{\cdot}H_2O$	0.00
$C_{84}H_{64}$	$H_3O^+{\cdot}H_2O$	0.21
$C_{84}H_{64}$	$O_2{\cdot}H_2O$	0.44
$C_{84}H_{64}$	$O_3{\cdot}H_2O$	0.51

TABLE 2 Electron transfer (ET) from NDs of varying sizes towards $O_2{\cdot}H_2O$, quantified by the transferred Hirshfeld charge in elemental unit charge e (PBE-D3/SVP geometries, TPSSH-D3/TZVP/CPCM[water] single point calculations)

ND	Adsorbates	ET/e
$C_{35}H_{36}$	$O_2{\cdot}H_2O$	0.30
$C_{53}H_{48}$	$O_2{\cdot}H_2O$	0.36
$C_{84}H_{64}$	$O_2{\cdot}H_2O$	0.44
$C_{147}H_{100}$	$O_2{\cdot}H_2O$	0.51

TABLE 3 Electron transfer (ET) from ND $C_{84}X_{64}$ (X = H,OH,F) to $O_2{\cdot}H_2O$, quantified by the transferred Hirshfeld charge in elemental unit charge e (PBE-D3/SVP geometries, TPSSH-D3/TZVP/CPCM[water] single point calculations)

ND	Adsorbates	ET/e
$C_{84}H_{64}$	$O_2{\cdot}H_2O$	0.44
$C_{84}(OH)_{64}$	$O_2{\cdot}H_2O$	0.31
$C_{84}F_{64}$	$O_2{\cdot}H_2O$	0.05

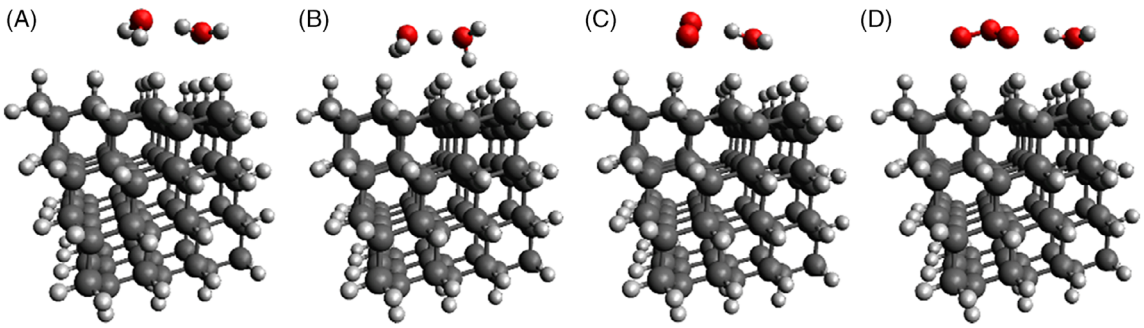

FIGURE 1 Structures of the nanodiamond (ND) $C_{84}H_{64}$ with different adsorbates: (A) $H_2O{\cdot}H_2O$, (B) $H_3O^+{\cdot}H_2O$, (C) $O_2{\cdot}H_2O$, (D) $O_3{\cdot}H_2O$. C atoms are depicted in black, O atoms in red, H atoms in light gray

consistent with earlier reports on transfer doping at bulk diamond.[28] We do not attempt to directly compare our results to those obtained for periodic surfaces, because different theoretical methods were used in the different studies, but, in general, the amounts of charge transfer obtained for NDs and the diamond (100) surface with the same adsorbates are similar in magnitude.[28]

The electron transfer properties for NDs of different sizes are shown in Table 2, the corresponding structures are shown in the SI, Figure S1. The adsorbate is $O_2{\cdot}H_2O$ in all calculations, as this is the most common oxidative species in ambient water. With increasing ND size, the amount of electron transfer increases from 0.30 e ($C_{35}H_{36}$) to 0.51 e ($C_{147}H_{100}$).

With larger ND sizes, their HOMOs shift to higher energies and the HLGs decrease. Accordingly, the energy difference between the ND HOMO and the adsorbate LUMO increases, because the adsorbate's LUMO is located at a relatively lower energy level. This results in an increased charge transfer from the ND HOMO to the adsorbate LUMO. The same effect was also found in previous work: The requirement for electron transfer is to have the adsorbate LUMO energetically below the substrate's HOMO (or valence band maximum), and increased charge transfer can be expected at higher energy differences.[26]

Table 3 contains the electron transfer properties of $C_{84}X_{64}$ with different surface terminations (X = H,F,OH), the respective structures and are shown in the SI, Figure S2. The amount of transfer doping is reduced by 30% when going from X = H to X = OH and reaches almost zero upon F termination. At the same time, the HOMO energies of the isolated NDs (obtained at the same level of theory) reduce from −5.39 eV (H) to −6.32 eV (OH) and further to −9.34 eV (F). Thus, with decreasing ND HOMO energy the amount of electron transfer to the adsorbate is reduced and finally annulled. While transfer doping in the presence of ozone at hydrogenated NDs may increase the oxidation rates, F-terminated NDs might be more stable under oxidizing conditions, because no additional hole doping occurs that potentially increases the NDs' reactivity. Fluorination of NDs may thus be an effective route for obtaining particles that are resistant to degradation in humid environment.

Further, we investigated the systems' frontier orbitals. In general, the orbitals of the respective system align as can be expected from the isolated ND's and adsorbates' orbital energies. For single spherical NDs in vacuum it is known that the LUMO and LUMOs + n (n = 1, 2, ...) are shaped like atomic orbitals (cf., following section).[34] The same orbital shapes, with slight distortions, are also found here in the presence of aqueous adsorbates at H-terminated NDs (not shown). In electron transfer doping, the chemical interaction occurs between the respective ND's HOMO and adsorbate's LUMO, thus, the LUMOs of the NDs are not involved and do not change in their shape.

3.2 | Diamondoids: cluster formation

3.2.1 | Electronic structure

The electronic properties of diamondoids and small NDs have been investigated in numerous theoretical studies.[40,51,59–63] Also, experimental results are available which give direct evidence on the electronic properties, i.e., the optical gaps of these systems.[39–41] For diamondoid optical gap calculations, Han and Bester demonstrated the necessity of including zero-point energy gap renormalization (ZPR) corrections to the calculated diamondoid electronic structures to account for coupling to nuclear vibrations.[52] Here, we study the H-terminated diamondoid molecules, their dimers, and clusters of different diamondoids. These structures can be regarded as model systems for larger high-quality, H-terminated NDs which are used, i.e., in photocatalysis.

Table 4 summarizes the DFT-calculated HOMO, LUMO and HLG values of the monomers, the HLGs of the respective dimers, and the experimental optical gap values from different experiments.[39–41] In the first two experiments (referred to as exp. 1[39] and exp. 2[40]), optical absorption measurements are conducted on dilute gaseous species, while in the third experiment X-ray emission and absorption spectra are obtained from powders (exp. 3).[41] Note that for diamantane and

TABLE 4 Calculated (TPSSH-D3/ma-SVP) and experimental electronic properties of diamondoids: monomer highest occupied molecular orbital (HOMO) and lowest unoccupied molecular orbital (LUMO) energies, zero-point energy gap normalization (ZPR), and monomer and dimer HOMO-LUMO-gap energies (all in eV). The calculated HLGs that are compared with the experimental values are highlighted in bold

Name	Sum	PG	HOMO	LUMO	ZPR[52]	HLG	Dimer HLG	Optical gap exp. 1[39]	Optical gap exp. 2[40]	Optical gap exp. 3[41]
Adamantane	$C_{10}H_{16}$	T_d	−7.17	−0.03	−0.33	**6.81**	**6.57**	6.49	6.55	6.03
Diamantane	$C_{14}H_{20}$	D_{3d}	−6.77	−0.08	−0.12	**6.57**	**6.32**	6.40	6.47	5.82
Triamantane	$C_{18}H_{24}$	C_{2v}	−6.51	−0.18	−0.23	**6.10**	**6.01**	6.06	6.10	5.68
[123]Tetramantane	$C_{22}H_{28}$	C_2	−6.40	−0.19	−0.20	**6.01**	**5.89**	5.95	5.98	5.60–5.65
[121]Tetramantane	$C_{22}H_{28}$	C_{2h}	−6.32	−0.20	−0.26	**5.86**	**5.78**	6.10	6.15	5.60–5.65
[1(2)3]Tetramantane	$C_{22}H_{28}$	C_{3v}	−6.42	−0.23	−0.32	**5.87**	**5.77**	5.94	5.96	5.60–5.65
[1(2,3)4]Pentamantane	$C_{26}H_{32}$	T_d	−6.37	−0.27	−0.27	**5.83**	**5.64**	5.81	5.85	5.54
[1212]Pentamantane	$C_{26}H_{32}$	C_{2v}	−6.17	−0.20	−0.26	**5.71**	**5.62**	5.85	5.90	5.51
[12312]Hexamantane	$C_{26}H_{30}$	D_{3d}	−6.21	−0.23	−0.30	**5.68**	**5.56**	5.88	5.91	5.54

Note: Point group (PG) and sum formula are given for each molecule.

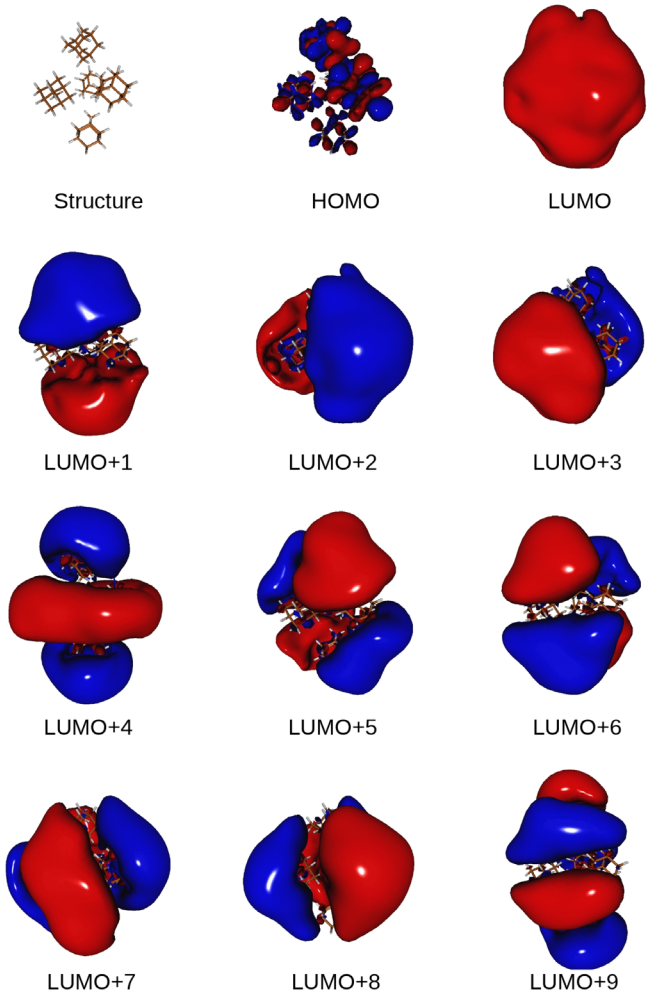

FIGURE 2 Structure, HOMO, LUMO and LUMOs + *n* of the $(adamantane)_5$ cluster (TPSSH-D3/ma-SVP). Contour surfaces of orbital amplitudes ±0.005. The orientation of the cluster is fixed in all frames

[121]tetramantane the DFT-HLGs are not a good approximation of the optical gap, because here the HOMO-LUMO transitions are symmetry-forbidden.

Adamantane has the highest optical gap, and the further gap values decrease with increasing size of the diamondoids according to the quantum size effect.[64] Upon dimer formation, the diamondoids' HLGs are reduced by 0.08–0.30 eV (0.16 eV on average). Generally, the ZPR-corrected HLGs of the monomers are in close agreement with the experimentally determined gaps obtained from diamondoid molecules in the gas phase (exp. 1 and 2). However, the optical gap values obtained from exp. 3 are up to 0.65 eV lower than those from exp. 1 and 2. This can be explained by the fact that exp. 3 used powders of the respective diamondoids instead of gas-phase molecules, and the formation of clusters results in a lowering of the respective gap values.

For larger cluster sizes the gap values further decrease and get closer to the optical gap values obtained from exp. 3. For example, our calculations results predict a gap decrease of 0.54 eV when going from single adamantane to the $(adamantane)_5$ cluster. The gap reduction originates in the lowering of the LUMO energies while the HOMO energies decrease only slightly. GW-corrected GGA-DFT calculations[65] showed that the gap value of crystalline adamantane is reduced by 0.6 eV as compared to the isolated molecule which is in good agreement with our results. The electronic structure changes of larger diamondoids' clusters are qualitatively the same as for adamantane.

3.2.2 | Frontier orbital shapes

Diamondoids and small NDs are known to have uniquely shaped frontier orbitals.[34,63] Especially, the LUMO and LUMOs + *n* (*n* = 1, 2, …) of spherical NDs resemble atom-type s, p, d, … orbitals. According to Han et al., these orbital shapes can generally be expected if (i) an outwards-pointing surface dipole is present, (ii) the system has spherical symmetry, and (iii) a dielectric mismatch exists between nanoparticle and vacuum.[34] In this work we investigate the corresponding orbitals of the diamondoid clusters to find very similar orbital shapes as for the single molecules.

Figure 2 shows the structure and contour plots of the HOMO, LUMO and LUMOs + *n* of the $(adamantane)_5$ cluster. All frontier MOs are delocalized over the whole cluster structure. The MOs' shapes are similar to those of the isolated adamantane molecule,[34,63] but stretched according to the shape of the cluster, clearly resembling atomic orbitals (LUMO: s, LUMO + (1–3): p, LUMO + (4–8): d, LUMO + 9: f). The same observation holds for the further diamondoid dimer and cluster structures: The HOMO, LUMO and LUMOs + *n* of the adamantane dimer and the hexamantane dimer are shown in the SI, Figures S3 and S4, respectively. Even mixed clusters of different diamondoid molecules have the same orbital characteristics, as we explicitly observed for the structures adamantane-hexamantane, triamantane-[1212]pentamantane and diamantane-[123]tetramantane-[1(2,3)4]pentamantane. The results clearly show that strict spherical symmetry of the system, the previous requirement (i),[34] is not necessary to observe these unique LUMO shapes. Instead, aggregates of both T_d-symmetrical and less symmetric diamondoids (e.g., [123]tetramantane, C_2) all show this type of LUMOs. We note here that clusters of rare gas atoms such as $(Ar)_4$ show the same type of joint LUMOs at this level of theory.

For the cases of dimers and clusters of identical diamondoids (non-mixed), also the HOMO and HOMOs − *n* (*n* ≥5) are delocalized among the respective molecules. For the mixed diamondoid aggregates, these orbitals are partly localized at one particular molecule and partly delocalized over several molecules. This confutes the previous assumption that no electron delocalization occurs between the different molecules of a cluster.[33]

4 | CONCLUSIONS

We have studied two examples of the effect of a condensed environment on the electronic structures of NDs. Firstly, we

investigated the effect of adding aqueous adsorbates ($H_2O{\cdot}H_2O$, $H_3O^+{\cdot}H_2O$, $O_2{\cdot}H_2O$, $O_3{\cdot}H_2O$) to small NDs of different sizes (35–147 C atoms) and surface terminations (H, OH, F). The combined results clearly prove that the concept of transfer doping remains valid for the case of nano-sized diamonds. The amount of charge transfer increases with the adsorbate's chemical potential and with the relative positioning of the ND's and adsorbate's frontier orbitals: With higher (lower) ND HOMO energies the effect is enhanced (decreased), which can be tuned via the ND's size and surface termination.

Secondly, we investigated changes of the electronic structure of diamondoids upon formation of dimers and larger clusters. With increasing size of the diamondoid molecules the HOMO energies increase significantly while the LUMO energies decrease only slightly. In contrast, upon cluster formation of adamantane, the system's HOMO energy increases only marginally and the decrease of the LUMO energies is more pronounced. In both cases, the optical gaps are reduced in larger systems. This explains the higher optical gap values that have been observed for the same diamondoids via measurements in vacuum[39,40] as compared to measurements conducted on powders.[41] Furthermore, we showed that the LUMO + n shapes of diamondoid clusters resemble atom-like orbitals, proving that electrons are delocalized among the molecules of a given cluster.

This work demonstrates that NDs should not be considered as inert particles when put in aqueous dispersions. Depending on their surface terminations, they strongly interact with oxidative species but also potentially with other O-containing molecules (proteins, chemical compounds) which may find applications in biology or catalysis. On the other hand, the NDs also strongly interact with each other when H-terminated, which can lead to aggregation but also modifies their optical properties. This has important implications, e.g., for ND photocatalysis, where the size of the ND's optical gap and its HOMO (or CBM) energy are crucial parameters of the catalytic process.[5,6] The precise interactions would require further experimental characterization in the future but should certainly be considered to gain a full picture of NDs' properties as colloidal solutions.

ACKNOWLEDGMENTS

TG and JD acknowledge the support of the Helmholtz Einstein International Berlin Research School in Data Science (HEIBRiDS). Most computations were carried out on the high-performance computing cluster CURTA by Zentraleinrichtung für Datenverarbeitung (ZEDAT) of Freie Universität Berlin.[66] Open Access funding enabled and organized by Projekt DEAL.

DATA AVAILABILITY STATEMENT

Data available on request from the authors. The data that support the findings of this study are available from the corresponding author upon reasonable request.

ORCID

Thorren Kirschbaum https://orcid.org/0000-0002-4120-3133
Tristan Petit https://orcid.org/0000-0002-6504-072X
Joachim Dzubiella https://orcid.org/0000-0001-6751-1487
Annika Bande https://orcid.org/0000-0003-3827-9169

REFERENCES

[1] V. N. Mochalin, O. Shenderova, D. Ho, Y. Gogotsi, *Nat. Nanotechnol.* **2012**, *7*(1), 11.
[2] A. Denisenko, A. Romanyuk, C. Pietzka, J. Scharpf, E. Kohn, *Diamond Relat. Mater.* **2010**, *19*(5), 423.
[3] J. H. T. Luong, K. B. Male, J. D. Glennon, *Analyst* **2009**, *134*(10), 1965.
[4] V. Acosta, P. Hemmer, *MRS Bull.* **2013**, *38*(2), 127.
[5] L. Zhang, D. Zhu, G. M. Nathanson, R. J. Hamers, *Angew. Chem., Int. Ed.* **2014**, *53*(37), 9746.
[6] D. Zhu, L. Zhang, R. E. Ruther, R. J. Hamers, *Nat. Mater.* **2013**, *12*(9), 836.
[7] C. G. Specht, O. A. Williams, R. B. Jackman, R. Schoepfer, *Biomaterials* **2004**, *25*(18), 4073.
[8] H. Huang, E. Pierstorff, E. Osawa, D. Ho, *Nano Lett.* **2007**, *7*(11), 3305.
[9] A. Alhaddad, M.-P. Adam, J. Botsoa, G. Dantelle, S. Perruchas, T. Gacoin, C. Mansuy, S. Lavielle, C. Malvy, F. Treussart, J.-R. Bertrand, *Small* **2011**, *7*(21), 3087.
[10] H. Wang, Y. Cui, *Carbon Energy* **2019**, *1*(1), 13.
[11] C.-Y. Ko, J.-H. Huang, S. Raina, W. P. Kang, *Analyst* **2013**, *138*(11), 3201.
[12] H. Etemadi, R. Yegani, V. Babaeipour, *J. Appl. Polym. Sci.* **2017**, *134* (21), 44873. https://doi.org/10.1002/app.44873
[13] C.-C. Chou, S.-H. Lee, *Wear* **2010**, *269*(11–12), 757.
[14] S. Aranifard, A. Shojaei, *Diamond Relat. Mater.* **2018**, *89*, 301.
[15] M. I. Landstrass, K. V. Ravi, *Appl. Phys. Lett.* **1989**, *55*, 4.
[16] H. Shiomi, Y. Nishibayashi, N. Fujimori, *Jpn. J. Appl. Phys.* **1991**, *30*, 1363. https://doi.org/10.1143/JJAP.30.1363
[17] V. Chakrapani, J. C. Angus, A. B. Anderson, S. D. Wolter, B. R. Stoner, G. U. Sumanasekera, *Science* **2007**, *318*(5855), 1424.
[18] J. A. Garrido, A. Härtl, M. Dankerl, A. Reitinger, M. Eickhoff, A. Helwig, G. Müller, M. Stutzmann, *J. Am. Chem. Soc.* **2008**, *130*(12), 4177.
[19] J. A. Garrido, S. Nowy, A. Härtl, M. Stutzmann, *Langmuir* **2008**, *24*(8), 3897.
[20] T. Petit, H. A. Girard, A. Trouvé, I. Batonneau-Gener, P. Bergonzo, J.-C. Arnault, *Nanoscale* **2013**, *5*(19), 8958.
[21] T. Petit, J.-C. Arnault, H. A. Girard, M. Sennour, T.-Y. Kang, C.-L. Cheng, P. Bergonzo, *Nanoscale* **2012**, *4*(21), 6792.
[22] O. Manelli, S. Corni, M. C. Righi, *J. Phys. Chem. C* **2010**, *114*(15), 7045.
[23] H. X. Young, Y. Yu, L. F. Xu, C. Z. Gu, *J. Phys.: Conf. Ser.* **2006**, *29*, 145.
[24] K. Larsson, J. Ristein, *J. Phys. Chem. B* **2005**, *109*(20), 10304.
[25] D. Petrini, K. Larsson, *J. Phys. Chem. B* **2005**, *109*(47), 6.
[26] Y. Takagi, K. Shiraishi, M. Kasu, H. Sato, *Surf. Sci.* **2013**, *609*, 203.
[27] M. M. Hassan, K. Larsson, *J. Phys. Chem. C* **2014**, *118*(40), 8.
[28] D. Petrini, K. Larsson, *J. Phys. Chem. C* **2007**, *111*(37), 9.
[29] J. Ristein, *Surf. Sci.* **2006**, *600*(18), 3677.
[30] J. Ackermann, A. Krueger, *Nanoscale* **2019**, *11*(16), 8012.
[31] S. L. Y. Chang, P. Reineck, D. Williams, G. Bryant, G. Opletal, S. A. El-Demrdash, P.-L. Chiu, E. Ōsawa, A. S. Barnard, C. Dwyer, *Nanoscale* **2020**, *12*(9), 5363.
[32] A. S. Barnard, *J. Mater. Chem.* **2008**, *18*(34), 4038.
[33] J. Hernández-Rojas, F. Calvo, *Front. Chem.* **2019**, *7*, 573. https://doi.org/10.3389/fchem.2019.00573
[34] P. Han, D. Antonov, J. Wrachtrup, G. Bester, *Phys. Rev. B* **2017**, *95*(19), 195428. https://doi.org/10.1103/PhysRevB.95.195428
[35] K. J. Rietwyk, S. L. Wong, L. Cao, K. M. O'Donnell, L. Ley, A. T. S. Wee, C. I. Pakes, *Appl. Phys. Lett.* **2013**, *102*(9), 091604. https://doi.org/10.1063/1.4793999

[36] S. Stehlik, T. Glatzel, V. Pichot, R. Pawlak, E. Meyer, D. Spitzer, B. Rezek, *Diamond Relat. Mater.* **2016**, *63*, 97.
[37] T. Petit, L. Puskar, T. Dolenko, S. Choudhury, E. Ritter, S. Burikov, K. Laptinskiy, Q. Brzustowski, U. Schade, H. Yuzawa, M. Nagasaka, N. Kosugi, M. Kurzyp, A. Venerosy, H. Girard, J.-C. Arnault, E. Osawa, N. Nunn, O. Shenderova, E. F. Aziz, *J. Phys. Chem. C* **2017**, *121*(9), 5185.
[38] A. Krueger, D. Lang, *Adv. Funct. Mater.* **2012**, *22*(5), 890.
[39] L. Landt, K. Klunder, J. E. Dahl, R. M. K. Carlson, T. Moller, C. Bostedt, *Phys. Rev. Lett.* **2009**, *103*(4), 047402. https://doi.org/10.1103/PhysRevLett.103.047402
[40] M. Vörös, A. Gali, *Phys. Rev. B* **2009**, *80*(16), 161411. https://doi.org/10.1103/PhysRevB.80.161411
[41] T. M. Willey, C. Bostedt, T. van Buuren, J. E. Dahl, S. G. Liu, R. M. K. Carlson, R. W. Meulenberg, E. J. Nelson, L. J. Terminello, *Phys. Rev. B* **2006**, *74*(20), 205432. https://doi.org/10.1103/PhysRevB.74.205432
[42] J. P. Perdew, K. Burke, M. Ernzerhof, *Phys. Rev. Lett.* **1996**, *77*(18), 3865.
[43] A. Schäfer, H. Horn, R. Ahlrichs, *J. Chem. Phys.* **1992**, *97*(4), 2571.
[44] F. Weigend, R. Ahlrichs, *Phys. Chem. Chem. Phys.* **2005**, *7*(18), 3297.
[45] J. P. Perdew, S. Kurth, A. Zupan, P. Blaha, *Phys. Rev. Lett.* **1999**, *82*(12), 2544.
[46] J. P. Perdew, J. Tao, V. N. Staroverov, G. E. Scuseria, *J. Chem. Phys.* **2004**, *120*(15), 6898.
[47] L. Goerigk, S. Grimme, *Phys. Chem. Chem. Phys.* **2011**, *13*(14), 6670.
[48] D. López-Carballeira, T. Polcar, *Diamond Relat. Mater.* **2020**, *108*, 107959. https://doi.org/10.1016/j.diamond.2020.107959
[49] V. Barone, M. Cossi, *J. Phys. Chem. A* **1998**, *102*(11), 1995.
[50] S. Grimme, A. Hansen, *Angew. Chem., Int. Ed.* **2015**, *54*(42), 12308.
[51] T. Szilvási, A. Gali, *J. Phys. Chem. C* **2014**, *118*(8), 4410.
[52] P. Han, G. Bester, *New J. Phys.* **2016**, *18*(11), 113052. https://doi.org/10.1088/1367-2630/18/11/113052
[53] S. Grimme, S. Ehrlich, L. Goerigk, *J. Comput. Chem.* **2011**, *32*(7), 1456.
[54] F. Neese, F. Wennmohs, A. Hansen, U. Becker, *Chem. Phys.* **2009**, *356*(1), 98.
[55] F. Weigend, *Phys. Chem. Chem. Phys.* **2006**, *8*(9), 1057.
[56] F. Neese, F. Wennmohs, U. Becker, C. Riplinger, *J. Chem. Phys.* **2020**, *152*(22), 224108. https://doi.org/10.1063/5.0004608
[57] A. S. Barnard, M. Sternberg, *J. Mater. Chem.* **2007**, *17*(45), 4811.
[58] A. J. Bard, L. R. Faulkner, Electrochemical Methods. in *Fundamentals and Applications*, 3rd ed., John Wiley & Sons, New York **2001**.
[59] H. Yin, Y. Ma, X. Hao, J. Mu, C. Liu, Z. Yi, *J. Chem. Phys.* **2014**, *140*(21), 214315. https://doi.org/10.1063/1.4880695
[60] T. Demján, M. Vörös, M. Palummo, A. Gali, *J. Chem. Phys.* **2014**, *141*(6), 064308. https://doi.org/10.1063/1.4891930
[61] M. Vörös, T. Demjén, A. Gali, *MRS Proc.* **2011**, *1370*, mrss11-1370-yy02-07.
[62] B. Adhikari, M. Fyta, *Nanotechnology* **2014**, *26*(3), 035701. https://doi.org/10.1088/0957-4484/26/3/035701
[63] N. D. Drummond, A. J. Williamson, R. J. Needs, G. Galli, *Phys. Rev. Lett.* **2005**, *95*(9), 096801. https://doi.org/10.1103/PhysRevLett.95.096801
[64] T. M. Willey, C. Bostedt, T. van Buuren, J. E. Dahl, S. G. Liu, R. M. K. Carlson, L. J. Terminello, T. Möller, *Phys. Rev. Lett.* **2005**, *95*(11), 113401. https://doi.org/10.1103/PhysRevLett.95.113401
[65] T. Sasagawa, Z. Shen, *J. Appl. Phys.* **2008**, *104*(7), 073704. https://doi.org/10.1063/1.2986637
[66] L. Bennett, B. Melchers, B. Proppe, *Curta: A General-Purpose High-Performance Computer at ZEDAT*, Freie Universität Berlin, Berlin, Germany **2020**. https://doi.org/10.17169/refubium-26754

SUPPORTING INFORMATION

Additional supporting information may be found in the online version of the article at the publisher's website.

How to cite this article: T. Kirschbaum, T. Petit, J. Dzubiella, A. Bande, *J. Comput. Chem.* **2022**, *43*(13), 923. https://doi.org/10.1002/jcc.26849